

TU/e Faculty of Mechanical Engineering

Internship at University of Stuttgart

Semester 1: 2016-2017

Automation, analysis and improvement of an experimental setup for the measurement of anisotropic friction

DC 2017.028

Reinders, J.M.F. (0816951)

Supervisors: Dipl.-Ing. Simon Walker M.S. (INM, University of Stuttgart)
Prof.dr.ir. Remco I. Leine (INM, University of Stuttgart)
Prof.dr. Henk Nijmeijer (DC, Eindhoven University of Technology)

Eindhoven, February 2, 2017

Preface

This report is written as a result of my internship at the University of Stuttgart which is part of my mechanical engineering masters program at the Eindhoven University of Technology. The internship is executed at the Institute for Nonlinear Mechanics at the University of Stuttgart from September to December 2016.

I would like to thank Professor Remco I. Leine for receiving me at his institute and his help with the project. Furthermore, I would like to thank Simon Walker for his daily supervision and help with the project.

Abstract

At the Institute for Nonlinear Mechanics of the University of Stuttgart an experimental setup to measure friction is developed. This setup has some problems regarding convenience in use and the acquired data differs from the expected data. Therefore, this project is executed to automate the setup using Matlab and to transform the measured data to the desired data. To achieve the automation a GUI is created which is used to conduct experiments and to do the post processing. The problem regarding the measured data is caused by a non-orthonormal coordinate frame of the force sensor. Therefore, a transformation matrix is computed to transform the data in the non-orthonormal frame to the desired data in an orthonormal frame. During the project some other potential problems are identified which are briefly documented.

Contents

1	Introduction	1
2	Anisotropic friction	2
2.1	Explanation of anisotropic friction	2
2.2	Graphical description of friction force and direction	2
2.3	Summary	4
3	Experimental setup	5
3.1	Overview of experimental setup	5
3.2	Problems of the setup	6
3.3	Summary	7
4	Automation of the experiments	8
4.1	Old experimental procedure	8
4.2	Rotation of the specimen using Matlab	8
4.3	Data acquisition using Matlab	8
4.4	Fitting of the data	8
4.5	GUI for experiments	10
4.6	Summary	10
5	Data transformation	11
5.1	Problem description	11
5.2	Alignment of sensor	11
5.3	Summary	16
6	Other identified potential problems	17
6.1	Applied moments	17
6.2	Startup of experiment	18
6.3	Stribeck effect	19
6.4	Vibrations	19
6.5	Summary	20
7	Results of data transformation	22
7.1	Isotropic results	22
7.2	Anisotropic results	23
7.3	Summary	25
8	Conclusion and recommendations	26
8.1	Conclusion	26
8.2	Recommendations	26
A	Matlab implementation of the specimens rotation	28
B	Matlab implementation of the data acquisition	30
C	GUI for experiments	32
D	Applied moments	33

List of symbols

Symbol	Description	Unit
a	Parameter of superellipse defining the horizontal radius	-
\mathbf{A}_{IS}	3×3 Transformation matrix from frame S to frame I	-
b	Parameter of superellipse defining the vertical radius	-
\mathcal{C}	Force reservoir which contains the friction force in every sliding direction	-
\mathcal{D}	Direction set, contains all sliding directions for every friction force	-
${}^k\mathbf{e}_i^j$	Unit vector used for direction, i defines the direction in frame j and k defines in which frame it is expressed	-
f	Value to minimize for least squares fit	-
F	Constant (122880) which gives the relation between desired RPM and command value for servo controller	-
g	Constant for gravitational acceleration	[m/s ²]
$FFFFFFFF$	A hexadecimal number which relates to rotation velocity	-
I	Coordinate frame orthogonal to sensor housing	-
\mathbf{I}	Identity matrix	-
m_f	Mass used for applying a known force	[kg]
m	Parameter of superellipse describing the curve in x	-
n	Parameter of superellipse describing the curve in y	-
N	Number of points in measurements	-
N_{high}	Constant (16777216) used to compute velocity commands	-
N_{low}	Constant (1048576) used to compute velocity commands	-
P_1	Position 1 of laser used for vibration measurements	-
P_2	Position 2 of laser used for vibration measurements	-
S	Coordinate frame of sensor	-
V	Desired rotational velocity	[RPM]
V_{com}	Value to transform to hexadecimal representation for certain velocity	-
$\hat{\mathbf{v}}$	Unit vector of sliding direction	-
x	Direction	-
x_d	x coordinate for current sample of measured data	-
x_e	x coordinate of fit closest to current sample of measured data	-
y	Direction	-
y_d	y coordinate for current sample of measured data	-
y_e	y coordinate of fit closest to current sample of measured data	-
$\boldsymbol{\lambda}_f$	Friction force vector	[N]
λ_N^i	Force in normal direction in frame i	[N]
λ_r^i	Force in radial direction in frame i	[N]
λ_{scale}^i	Expected force in the given direction according to the scale	[N]
λ_t^i	Force in tangential direction in frame i	[N]
λ_{T_1}	Force in T_1 direction of the final body fixed frame	[N]
λ_{T_2}	Force in T_2 direction of the final body fixed frame	[N]
λ_x	x component of force vector $\boldsymbol{\lambda}_f$	[N]
λ_y	y component of force vector $\boldsymbol{\lambda}_f$	[N]
${}_S\boldsymbol{\lambda}_i^I$	Vector of measured forces in frame S when force λ is applied in direction i of frame I	[N]
φ	Angle of rotation of disc	[rad]
$0W$	Command to write data to servo controller	-
$00E3$	Command to set rotation speed using the RS-232 port	-

1 Introduction

At the Institute for Nonlinear Mechanics (INM) of the University of Stuttgart an experimental setup is developed. This setup is used for measurements of friction, specifically anisotropic friction. The setup is used in a project with the aim to establish a valid description of anisotropic friction [1]. It is used to measure the components (radial and tangential direction) of the anisotropic friction force for different sliding directions. With this data the normal cone inclusion force law for anisotropic friction is investigated and the shape of force reservoirs is analyzed [1]. The developed setup is a pin on disc setup, this setup is ideal in the sense that for one full rotation the friction force in every sliding direction is measured. However, the developed setup has various issues. Firstly, multiple software programs are used when taking measurements and doing the post processing. This makes working with the setup time consuming and inconvenient. Furthermore, the measured forces using the force sensor are not as expected. In this project these issues are solved and there is looked into other possible issues of the setup. This gives the main goal of the project: Automating and improving the experimental setup. The problem of automating the setup consists of two problems. First of all the rotation of the disc is automated using Matlab and secondly the data acquisition is automated using Matlab. To improve the setup the measured forces are transformed to the desired forces. To achieve the goals of the project, first of all there is a brief description of anisotropic friction in Chapter 2. Thereafter, in Chapter 3 the setup is shown and the main problems are stated and described more extensively. Then, in Chapter 4 the first goal, the automation of the experimental setup is addressed. This goal is achieved by designing a graphical user interface (GUI) in Matlab. Thereafter, in Chapter 5 the improvement of the setup is explained by transforming the measured forces to the desired forces. During the project some other possible problems are identified, these open problems are briefly described in Chapter 6. To compare measurements while using the new data transformation and without it Chapter 7 shows the obtained results using the data transformation. Finally, some conclusions and recommendations for further research are given.

2 Anisotropic friction

In this chapter first of all, an explanation of anisotropic friction is given. After that, the way of describing anisotropic friction in a 2-D plane using concepts from convex analysis is explained.

2.1 Explanation of anisotropic friction

Anisotropic friction occurs due to surface texture of a material. An example of this is surface ground steel where all the scratches are in one direction, which results in different friction forces for different sliding directions, see Figure 2.1 [2]. But also materials in nature like crystalline solids or organic materials such as wood have an anisotropic structure. When a body is moving over such a surface with no force working on it except for the friction force it will deflect from its straight path depending on the orientation with respect to the surface texture. Because the only force acting on the sliding body is the friction force this means that the deflection is caused by the friction force. So the friction force is not in exact opposite direction of the velocity, see Figure 2.2. The deflection in this figure is different for different sliding directions. Thus, the direction of the friction force is dependent on the orientation of the scratches with respect to the sliding direction. Furthermore, the magnitude of the force is also dependent on the sliding direction. For example, when an object is sliding along the scratches the friction force has a different magnitude then when the object slides orthogonal to the scratches.

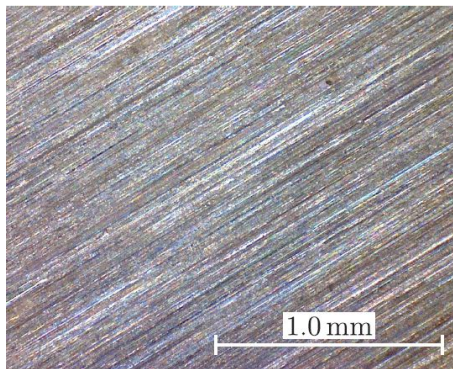


Fig 2.1: Microscopic view of surface ground steel, it clearly shows that the scratches are oriented in the same direction [2].

2.2 Graphical description of friction force and direction

For the graphical representation of the friction force in every sliding direction of an isotropic surface a force set can be drawn by assuming that there is Coulomb friction. Coulomb friction means that the friction force has a certain constant value (in opposite direction of the velocity) when moving and the value is between those constant values when not in motion (stiction), see Figure 2.3a. Because it is assumed for the isotropic case that the force in every direction has the same magnitude, the isotropic friction reservoir (\mathcal{C}) can be visualized as shown in Figure 2.3b. In this figure the friction force is described by vector λ_f and the sliding direction corresponding to this force is perpendicular to set \mathcal{C} , thus $\hat{\mathbf{v}}$. This shows that the magnitude of the force is the same in every sliding direction and exactly in opposite direction of the velocity. During stiction the friction force is somewhere inside the red circle.

Because in the anisotropic case the magnitude of the friction force is not the same for every sliding direction and the direction of the force is not always in opposite direction of the velocity another representation is used. A new set is introduced called the direction set \mathcal{D} . The sets \mathcal{C} and \mathcal{D} together describe the friction force in all sliding directions, an example is shown in Figure 2.4. In this figure two sets are shown, the red force reservoir \mathcal{C} which gives the magnitude and direction of the friction force and set \mathcal{D} which gives the sliding direction of the object. When drawing

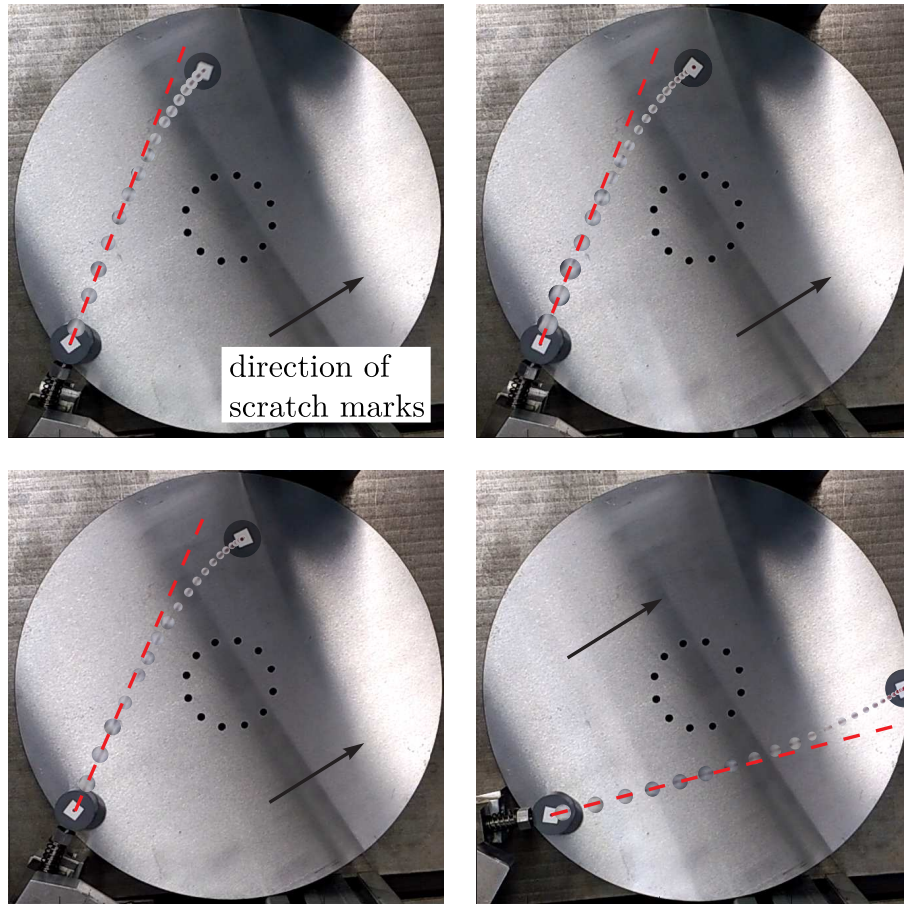
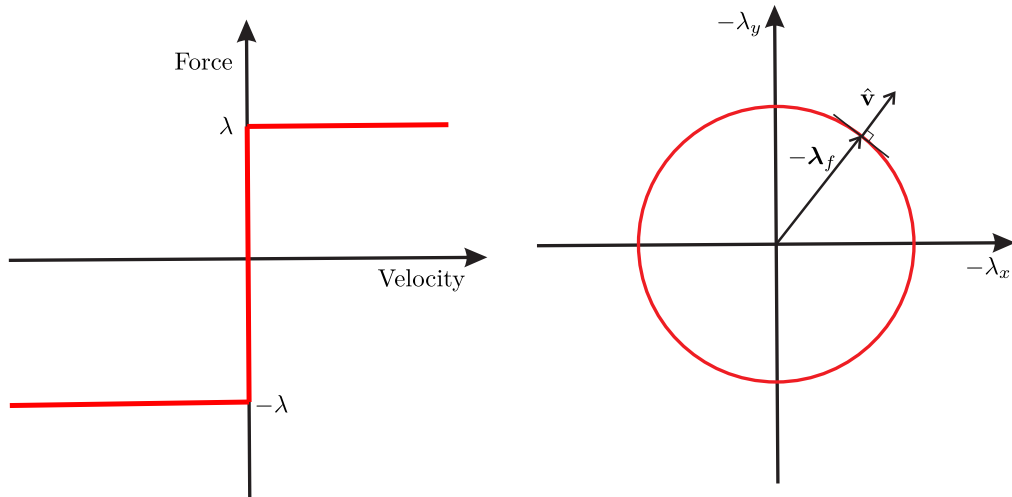


Fig 2.2: Block sliding over anisotropic surface, the figure clearly shows a deflection of the sliding body dependent on sliding direction. The scratches are in the direction of the black arrow [2].



(a) Coulomb friction force against velocity, when moving the force is λ in opposite direction of the sliding velocity. When not moving the force is between $-\lambda$ and λ .

(b) Friction force in x and y direction for every sliding direction in isotropic case. The friction force is given by λ_f and the corresponding sliding direction is perpendicular to the edge of set \mathcal{C} (red circle), thus \hat{v} .

Fig 2.3: Friction force in isotropic case.

the negative force vector from the origin to the edge of the force reservoir the sliding direction is obtained by the vector perpendicular to set \mathcal{D} where the negative force vector crosses it.

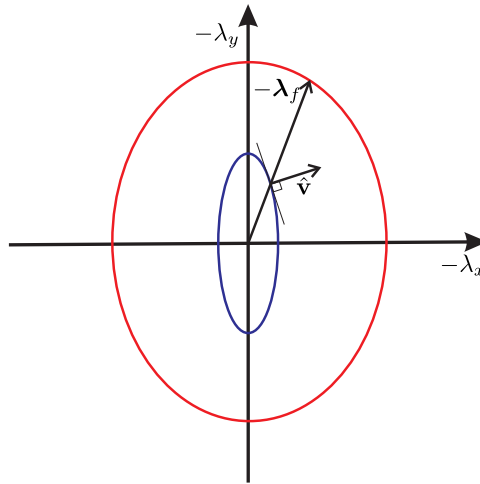


Fig 2.4: Sets \mathcal{C} (red ellipse) and \mathcal{D} (blue ellipse) for the anisotropic case and the corresponding force and direction vector.

2.3 Summary

In this chapter an explanation of anisotropic friction is given. In the case of anisotropic friction the magnitude and direction of the friction force are dependent on the sliding direction. Furthermore, a graphical description of anisotropic friction is given for every sliding direction using a force reservoir \mathcal{C} and direction set \mathcal{D} , see Figure 2.4.

3 Experimental setup

This chapter gives an overview of the experimental setup realized at INM, see Figure 3.1. First of all a brief overview is given of what it does, then the individual components are briefly discussed and finally some improvements are suggested which are discussed in the remainder of the report.

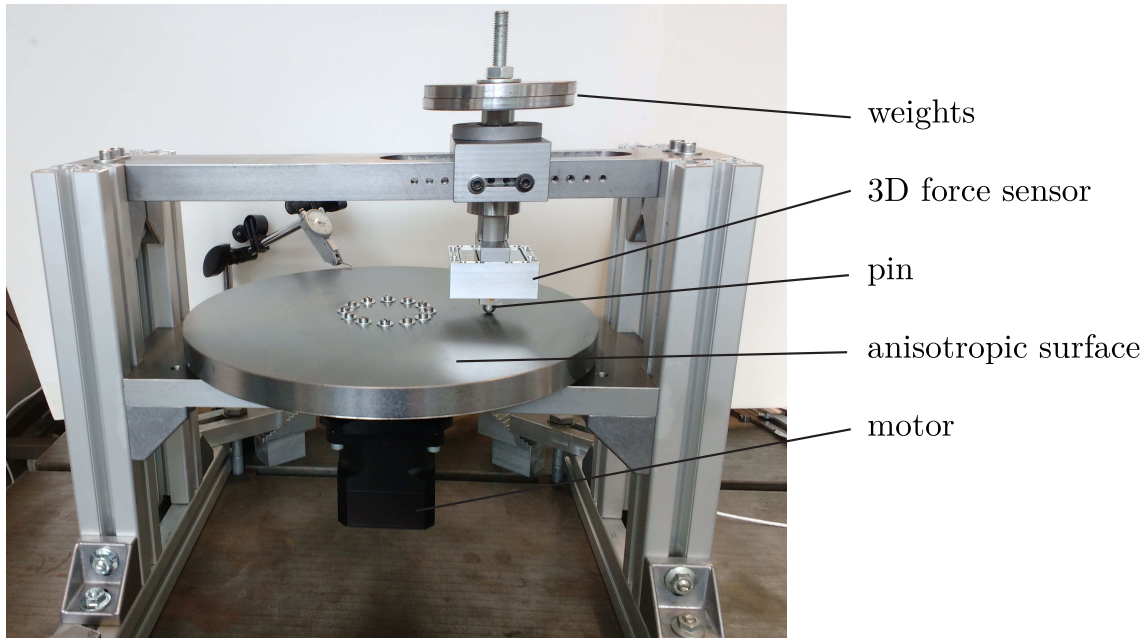


Fig 3.1: The experimental setup with its most important parts [2].

3.1 Overview of experimental setup

The purpose of the setup is to measure the contact force in three spatial directions, which are used to analyze anisotropic friction. For the 3D force sensor these are the radial (λ_r), tangential (λ_t) and normal (λ_N) force, the directions are shown in Figure 3.2. Using the known rotation (φ) it is possible to transform the measured forces to the body fixed coordinate frame which is rotating with the plate, for more information on this see [2]. Using these transformed coordinates, the sets \mathcal{C} and \mathcal{D} of the specimen are computed.

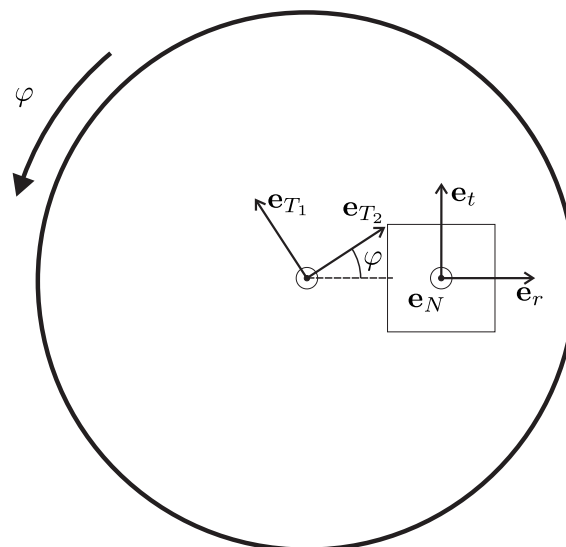


Fig 3.2: Sketch of the top view of the setup with the used coordinate frames.

The main components of the setup are shown in Figure 3.1. The most important part in this picture is the 3D force sensor (ME-Meßsysteme K3D60), which is measuring the contact force acting on the pin in three spatial directions. An excitation voltage is going into the force sensor and due to forces acting on it, resistors stretch or get compressed which changes the resistance. The change of the output voltage is amplified by the amplifier. The resulting voltage is converted to a force in Newton by the data acquisition device (DEWE-BOOK) which shows the live data on the computer using DeweSoft. After an experiment this data is retrieved from DeweSoft for post processing. A schematic overview of the data flow is shown in Figure 3.3.

The specimen that is examined (in the case of the picture the surface ground steel plate) is easily replaceable or another plate can be placed on top of the anisotropic surface. Furthermore, the pin which is used to create the contact between the force sensor and the specimen is also easy to replace, this way different pins made out of different materials and with different shapes can be used.

The specimen is rotated by the motor which has its own servo-controller which keeps it rotating at constant rotational velocity. The desired velocity is send to the servo-controller using the related software (ServoCommander) on the computer. Furthermore, the servo-controller keeps track of the rotational angle which is send to the DEWE-BOOK for post processing. The motor uses a harmonic drive unit with a gear ratio of 30 to 1 to transfer its torque to the specimen.

Finally, At the top of the picture weights are shown. These can easily be taken of or more weights can be added to see the effect of a different normal force.

There is another possible option to measure friction forces. This alternative uses a pin which slides in a straight line over the surface. The biggest advantage of the pin on disc setup over the alternative is that in one rotation the friction force in every sliding direction is measured. With the method of a pin sliding in a straight line a lot of measurements have to be conducted to get information about all sliding directions.

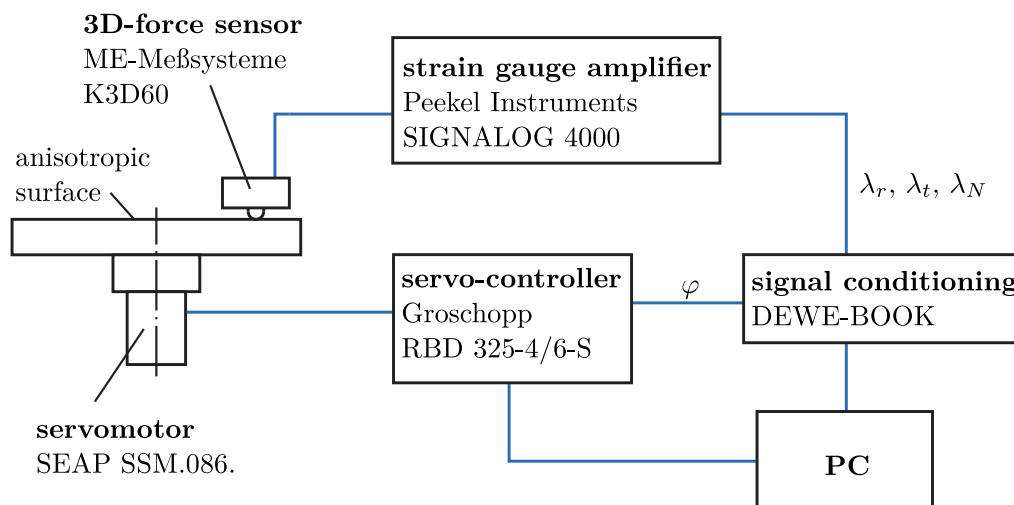


Fig 3.3: Schematic overview of the data flow. The data flow between the force sensor, amplifier, DEWE-BOOK, servo-controller, servomotor and computer.

3.2 Problems of the setup

The first problem is the time-consuming process of taking measurements. When everything is turned on and ready to start first of all DeweSoft, the software program for the DEWE-BOOK is turned on and data-acquisition is started. After this, ServoCommander is used to send commands to the servo-controller to start spinning. Then, the motor and the data-acquisition both are stopped using ServoCommander and DeweSoft again. After this, the obtained data is exported as a '.mat' file to use it in Matlab for the post processing. To simplify this a GUI is designed which makes this process more convenient and less time-consuming.

The next problem is the obtained data from measurements, when an experiment is conducted for

a full rotation the mean of the radial force measured by the sensor is expected to be zero thus

$$\int_0^{2\pi} \lambda_r^S d\varphi \approx 0, \quad (3.1)$$

should hold. This should hold because it is assumed that the surface is orthotropic and symmetric (the radial force after π radians of rotation is the same but in opposite direction, thus they cancel each other). In previous experiments it is clearly seen that this is not the case. This is probably caused by a faulty sensor or a misalignment of the sensor in respect to the specimen.

Furthermore, the sensor is used to measure forces however, it is not a force that is acting on the sensor but a moment. It is investigated if this influences the acquired data. During the use of the setup some other problems are observed, these are also briefly discussed later in this report.

3.3 Summary

This chapter showed the experimental setup and its most important parts are described more extensively. It also explained how the setup is used to determine the force reservoir and direction set. Furthermore, the biggest problems are explained. These problems are the time-consuming process of taking measurements and the measured data which does not correspond to the expected data.

4 Automation of the experiments

This chapter discusses the automation of the experiments. In the first section it is briefly explained how the experiments are conducted. This is done to get an overview of what is needed for the automation. Thereafter, it is explained how the individual components (rotation of the specimen and data acquisition) are automated using Matlab. Then the implemented fitting tool for the obtained data sets is explained. Finally, it is discussed how this is brought together into one GUI using Matlab.

4.1 Old experimental procedure

All the experiments start with the pin (and sensor) lifted from the surface of the specimen. First of all the software programs DeweSoft and ServoCommander are started. Next, a setup is loaded into DeweSoft which tells it which channels of the DEWE-BOOK to use. Then, while the pin is lifted the values for the forces are reset to 0. Thereafter, the pin is dropped to make contact with the specimen. Then, the data acquisition is started using DeweSoft. Thereafter, the motor is started to spin at a constant velocity using ServoCommander. When the desired number of rotations is achieved the motor and data acquisition are manually stopped and the data is exported for post processing in Matlab. This is a time consuming and devious process because a lot of different software programs are used. The goal is to do everything from loading the setup until post processing within the Matlab environment using a convenient GUI.

4.2 Rotation of the specimen using Matlab

The servomotor which is used to rotate the specimen is controlled by a servo-controller. This servo-controller comes with a software program called ServoCommander. This program sends a desired rotational velocity to the servo-controller which keeps the motor rotating at constant velocity until ServoCommander sends a command with a different velocity. To do this using Matlab instead of using ServoCommander a command is sent from Matlab to the servo-controller using the RS-232 port. How this is implemented is explained in Appendix A.

There is room for improvement, the number of rotations is not exactly equal to the desired number of rotations. This is caused by the counter in Matlab which is not perfect and by acceleration and deceleration which are not taken into account when computing the desired rotation time.

4.3 Data acquisition using Matlab

In addition to controlling the rotation of the specimen with Matlab, the measured data has to be acquired using Matlab. This is achieved using the data acquisition device DEWE-BOOK and the software program DeweSoft. The program DeweSoft comes with DCOM commands which are commands that Matlab can send to the program to control it. These commands can be found in the DeweSoft DCOM manual [4]. The implementation of data acquisition in Matlab is given in Appendix B.

4.4 Fitting of the data

To get a smooth representation and a function to describe the force reservoir (\mathcal{C}) and the set of directions (\mathcal{D}) a fitting tool is added to the post processing. The fitting is done using a least squares optimization with a superellipse.

Because a normal ellipse might not be the best description (sometimes the data shows a square with rounded edges) superellipses are used instead. Instead of just parameters for the radii it also has parameters related to the curvature in both directions. If this parameter is very high it shows a square with rounded edges (see Figure 4.1). The equation of a superellipse is given as

$$\left|\frac{x}{a}\right|^m + \left|\frac{y}{b}\right|^n = 1, \text{ with } m, n > 0, \quad (4.1)$$

in this equation x and y are the coordinates, a and b are the radii of the ellipse and m and n are parameters which give the roundness of the curve. This can be rewritten to equations for the x and y coordinates as follows

$$x(\theta) = |\cos(\theta)|^{\frac{2}{m}} a \operatorname{sgn}(\cos(\theta)), \quad (4.2)$$

$$y(\theta) = |\sin(\theta)|^{\frac{2}{n}} b \operatorname{sgn}(\sin(\theta)), \quad (4.3)$$

with θ a parameter between 0 and 2π on the curve (not the physical angle). In Figure 4.1 three different superellipses are shown with constant values for a and b but different values for m and n , this figure shows the influence of those parameters.

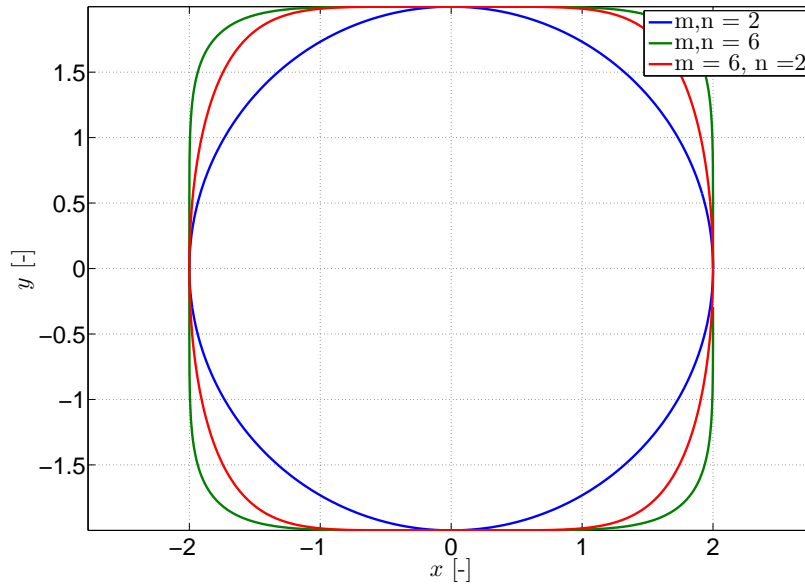


Fig 4.1: Superellipses for different parameters to show the influence of m and n , a and b are constant at 2.

To get the best fit of the measured data a least squares optimization is done. The optimization problem is described as follows

$$\begin{aligned} \min_{m,n,a,b} f(m,n,a,b) &= \frac{1}{N} \sum_{i=1}^N \sqrt{(x_d(i) - x_e(m,n,a,b))^2 + (y_d(i) - y_e(m,n,a,b))^2} \\ \text{s.t.} & \\ m,n,a,b &> 0, \end{aligned} \quad (4.4)$$

with m, n, a, b the parameters of the ellipse as given before, (x_e, y_e) the point of the fit closest to the measured point $(x_d(i), y_d(i))$ and N the number of samples of the measurement which are used for the fit. This optimization minimizes the mean distance between the points of the measured data and the fitted ellipse with the only constrained that all the parameters are greater then 0. All of this is implemented in Matlab using the function *Fmincon* a result of this is shown in Chapter 7.

4.5 GUI for experiments

To make it easy and fast to use the setup, a Matlab GUI is created which combines the previously mentioned steps for the experiments and also includes the post processing. Figure C.1 shows an image of the GUI. To use the GUI (See Figure 4.2), first of all the desired translational velocity, number of rotations, sample rate and the measured radius have to be inserted. Then, a choice has to be made if data has to be acquired or not. If not the button just spinning can be used to make the turning table rotate. If data has to be acquired a setup has to be chosen and loaded, a save name has to be chosen and the sensor has to be set to zero. After this, the pin has to be dropped on the specimen. Thereafter, the start measurement button can be used to start the measurement. Finally, the obtained data (or previously obtained data) can be used for post processing. For post processing the part of the measurement which is used has to be chosen by choosing the start and end angle in radians. Furthermore, an angle can be chosen to rotate the obtained sets \mathcal{C} and \mathcal{D} for plotting and fitting purposes. The box fit ellipse can be used to fit ellipses on the obtained sets. In case of emergency a stop button is included to terminate the experiment immediately. There is room for improvement of the GUI. For example, a homing button could be added to move the specimen to a fixed starting position before experiments.

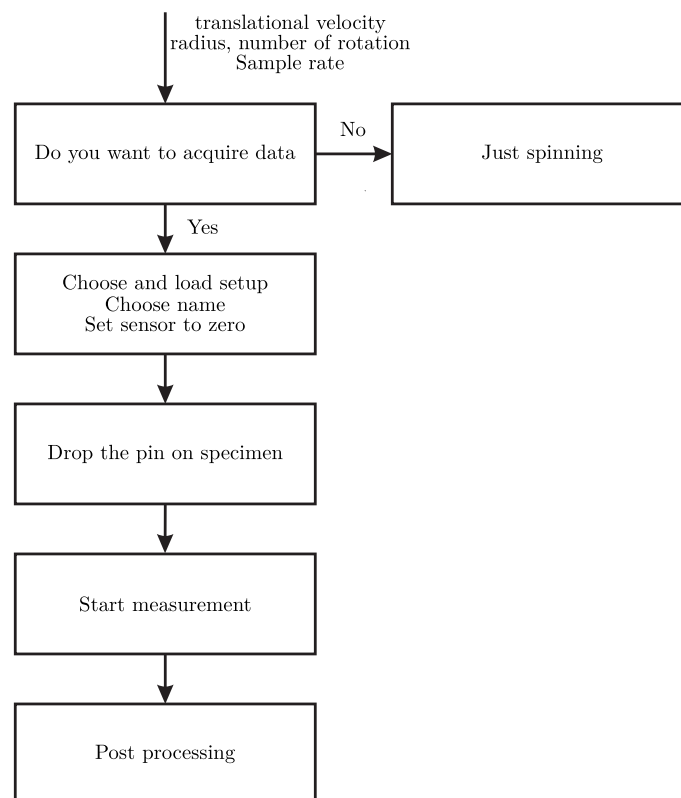


Fig 4.2: Flowchart on how to conduct a measurement using the GUI in Matlab.

4.6 Summary

This chapter describes the experimental procedure which is very time consuming because multiple software programs are used. Therefore, an automation of the experiments is needed. First, the automation of the specimens rotation in Matlab is discussed using a direct connection with the servo-controller over the RS-232 port. Thereafter, automation of the data acquisition using DCOM commands in Matlab is explained. Furthermore, a fitting tool for the obtained sets \mathcal{C} and \mathcal{D} using superellipses is described. Then, the created GUI is explained in which these functions are combined and post processing is added. Finally, some suggestions for improvements are done, namely making the specimen stop at exactly the desired number of rotations and adding a homing function.

5 Data transformation

This chapter discusses the transformation from raw data measured in the sensor frame to useful data in the desired frame. As mentioned in Chapter 3 there is a problem with the sensor. In this Chapter a more elaborate description and a solution of this problem are given.

5.1 Problem description

The obtained data from measurements shows inconsistency with the expectations. When measurements are done there are forces in three directions desired as shown in Figure 3.2. For an isotropic surface it is expected that the radial force (λ_r) is around zero in every direction. For anisotropic surfaces the integral of this force should be zero over a full number of rotations (assumed that the surface is orthotropic and symmetric). But the data from measurements of an isotropic surface shows a constant force in radial direction, see Figure 5.1. For this measurement a brass pin on a sandblasted steel plate is used and the sliding velocity is 150 mm/s. This figure clearly shows a non zero value for the radial force. Therefore, it is assumed that there is probably some kind of misalignment of the sensor and due to this misalignment some of the normal and/or the tangential force is measured in the radial direction.

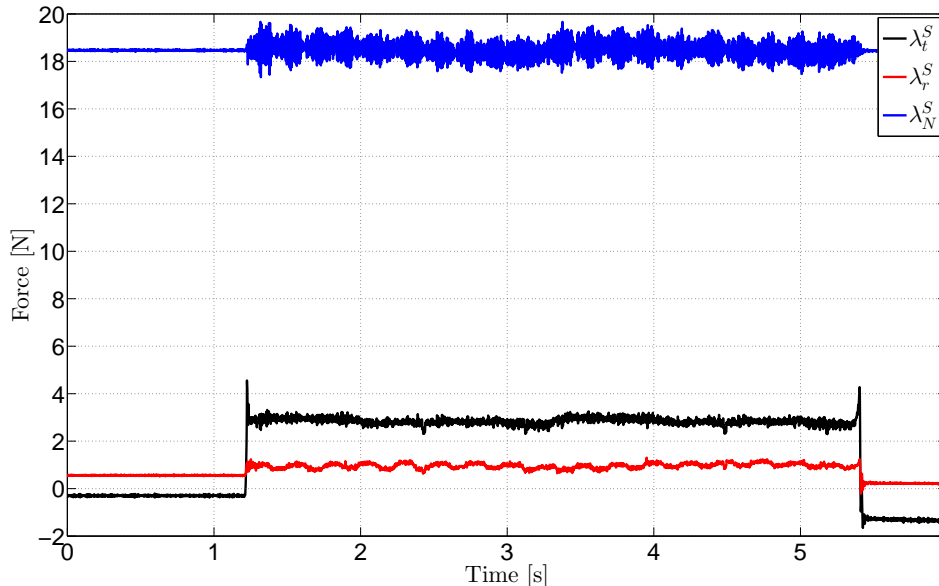


Fig 5.1: Raw measured forces over about two rotations of an isotropic surface.

5.2 Alignment of sensor

For the alignment of the sensor different approaches are tested. At first it is assumed that the alignment of the sensor in respect to the specimen is not perfect. This would mean that a constant rotation of the measured data should be enough to solve the problem. But this did not give a satisfying solution.

Therefore tests are conducted with the sensor. Different known forces are applied purely in one direction in the I frame as given in Figure 5.2, the I frame is the frame orthogonal to the sensor housing. These forces are applied by using a known mass and hanging this from the sensor in \mathbf{e}_t^I , \mathbf{e}_r^I and \mathbf{e}_N^I direction. The resulting forces in the sensor frame S are measured and plotted, which should result in a force purely in the desired direction in the S frame. The results of this experiment are shown in the Figures 5.3, 5.4 and 5.5 which respectively show the experiment with the force exerted in \mathbf{e}_t^I , \mathbf{e}_r^I and \mathbf{e}_N^I direction. These figures show that the calibration is fairly accurate, the difference between the applied force, which in the figures is represented by (λ_{scale})

and measured force is small, the biggest deviation is about 3.4 percent of the expected value. The interesting part is the fact that when the force is exerted in just \mathbf{e}_t^I and \mathbf{e}_N^I direction there is a proportional linear increase in λ_r^S , which might be caused by a constant rotation of the frame S with respect to frame I . But if a rotation is the case, there should be a proportional change in λ_N^S and λ_t^S when exerting a force in \mathbf{e}_r^I direction. This is not the case, which means that the sensor frame S is non-orthonormal, see Figure 5.2 and thus a rotation would not suffice.

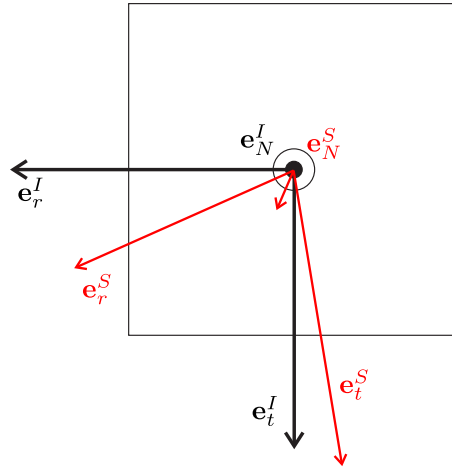


Fig 5.2: Sketch of the top view of the sensor, with the desired sensor frame I and a potential non-orthonormal sensor frame S .

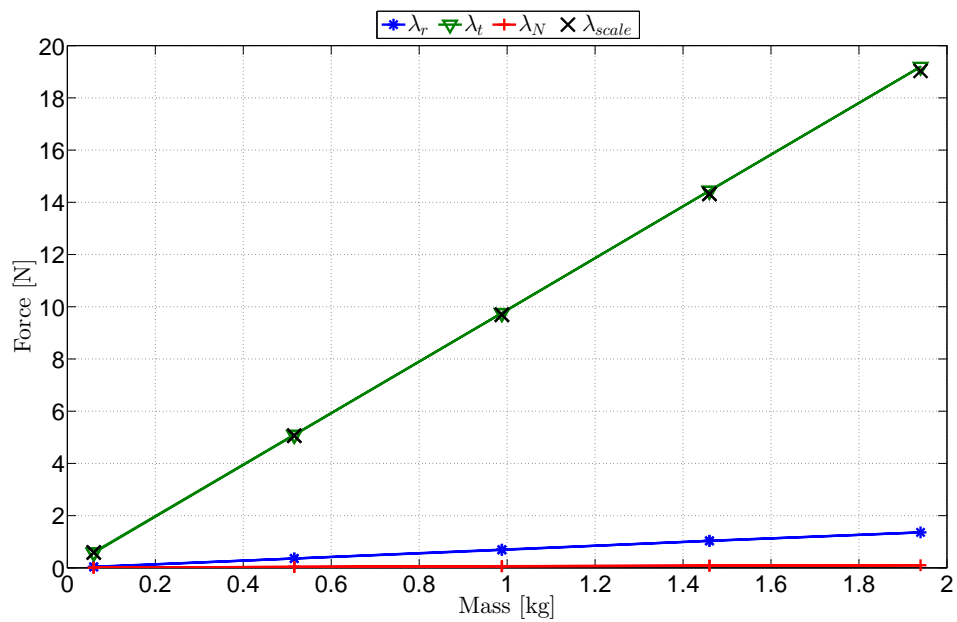


Fig 5.3: Forces measured in the S frame while forces are purely exerted in the \mathbf{e}_t^I direction.

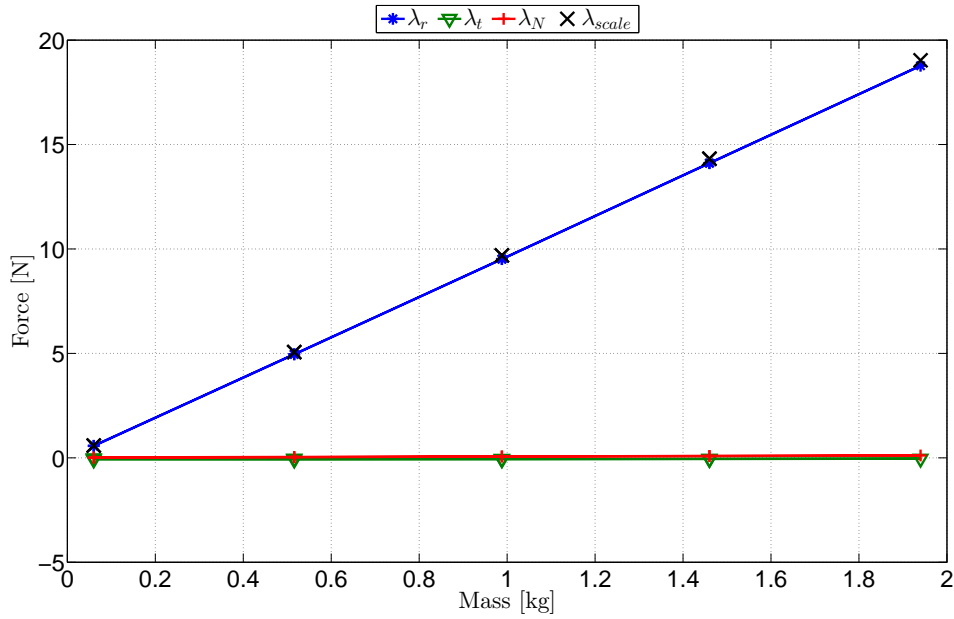


Fig 5.4: Forces measured in the S frame while forces are purely exerted in the \mathbf{e}_r^I direction.

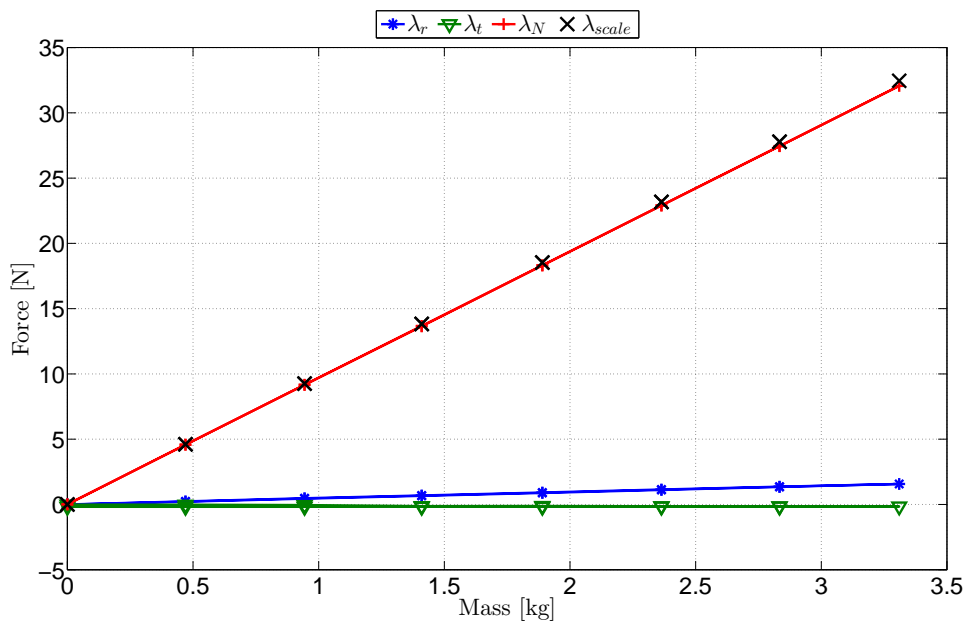


Fig 5.5: Forces measured in the S frame while forces are purely exerted in the \mathbf{e}_N^I direction.

Because the frame of the sensor is not orthonormal a rotation matrix would not suffice therefore another approach is needed. The goal is to find a transformation matrix \mathbf{A}_{IS} which transforms a force vector $\boldsymbol{\lambda}$ expressed in frame S to a vector expressed in frame I . Thus

$${}_I\boldsymbol{\lambda} = \mathbf{A}_{IS} {}_S\boldsymbol{\lambda}, \quad (5.1)$$

with ${}_i\boldsymbol{\lambda}$ the force vector $\boldsymbol{\lambda}$ expressed in frame i . This matrix can also be used to transform the frame S to frame I as follows

$$\mathbf{I} = ({}_I\mathbf{e}_r \quad {}_I\mathbf{e}_t \quad {}_I\mathbf{e}_N) = \mathbf{A}_{IS} ({}_S\mathbf{e}_r^I \quad {}_S\mathbf{e}_t^I \quad {}_S\mathbf{e}_N^I), \quad (5.2)$$

$$\mathbf{A}_{IS} = ({}_I\mathbf{e}_r^S \quad {}_I\mathbf{e}_t^S \quad {}_I\mathbf{e}_N^S), \quad (5.3)$$

in this equation ${}_k\mathbf{e}_i^j$ is the direction i of frame j expressed in frame k . Applying a known force (using a mass) in these known directions of the I frame results in a measured expression of this force in the S frame. This is done in all three direction of frame I which results in three force vectors measured in frame S and results in the following

$$\begin{pmatrix} \lambda_r^I & 0 & 0 \\ 0 & \lambda_t^I & 0 \\ 0 & 0 & \lambda_N^I \end{pmatrix} = \mathbf{A}_{IS} ({}_S\lambda_r^I \quad {}_S\lambda_t^I \quad {}_S\lambda_N^I), \quad (5.4)$$

with ${}_S\lambda_i^I$ the force measured in frame S with force λ is applied in \mathbf{e}_i^I direction. Because the applied force is known and equal in every direction this is rewritten to

$$m_f g \mathbf{I} = \mathbf{A}_{IS} ({}_S\lambda_r^I \quad {}_S\lambda_t^I \quad {}_S\lambda_N^I), \quad (5.5)$$

with m_f the used mass, g the gravitational acceleration constant (9.81 m/s²) and \mathbf{I} a 3×3 identity matrix. Because the applied forces are known and the forces are measured in the S frame, \mathbf{A}_{IS} is obtained by rewriting 5.5 to the following

$$\mathbf{A}_{IS} = \left(\frac{1}{m_f g} ({}_S\lambda_r^I \quad {}_S\lambda_t^I \quad {}_S\lambda_N^I) \right)^{-1}, \quad (5.6)$$

which results in the desired matrix \mathbf{A}_{IS} .

By doing four experiments in both positive and negative directions of the frame I and taking the mean of this the matrix is computed. The biggest deviation between matrix entries for the different experiments is about 0.02. The resulting matrix is

$$\mathbf{A}_{IS} = \begin{pmatrix} 1.0174 & -0.0770 & -0.0408 \\ 0.0004 & 0.9911 & 0.0013 \\ -0.0038 & 0.0022 & 1.0083 \end{pmatrix}. \quad (5.7)$$

If the calibration would be perfect and the directions of the sensor frame would be orthogonal to the sensor housing, the matrix would be the identity matrix. The obtained matrix shows values on the diagonal close to one and values close to zero on most off-diagonal entries. It shows that the off-diagonal entries in the first row contain fairly high values this is because the radial component increased linearly when increasing the applied tangential and normal force. Thus, a value which is related to these forces is subtracted to compensate for this linear increase. The other values are all close to zero because there is a very small influence of other forces on the tangential and radial force.

When the forces in Figures 5.3, 5.4 and 5.5 are premultiplied with this matrix the Figures 5.6, 5.7 and 5.8 are obtained. Comparing these figures clearly shows that the linear dependency of directions in which no force is exerted is much smaller. Furthermore, the calibration is better, the scale value is closer to the measured value in frame I . It is not perfect, this might be caused by a transformation matrix that is not perfect yet or forces which are not exerted perfectly orthogonal to the sensor housing. But for now it is assumed to be adequate. The results of measurements using this transformation matrix and the difference with measurements without this transformation are shown in Chapter 7. Now the measured data can be transformed from frame S to frame I it is trivial to transform the data to the frame in Figure 3.2.

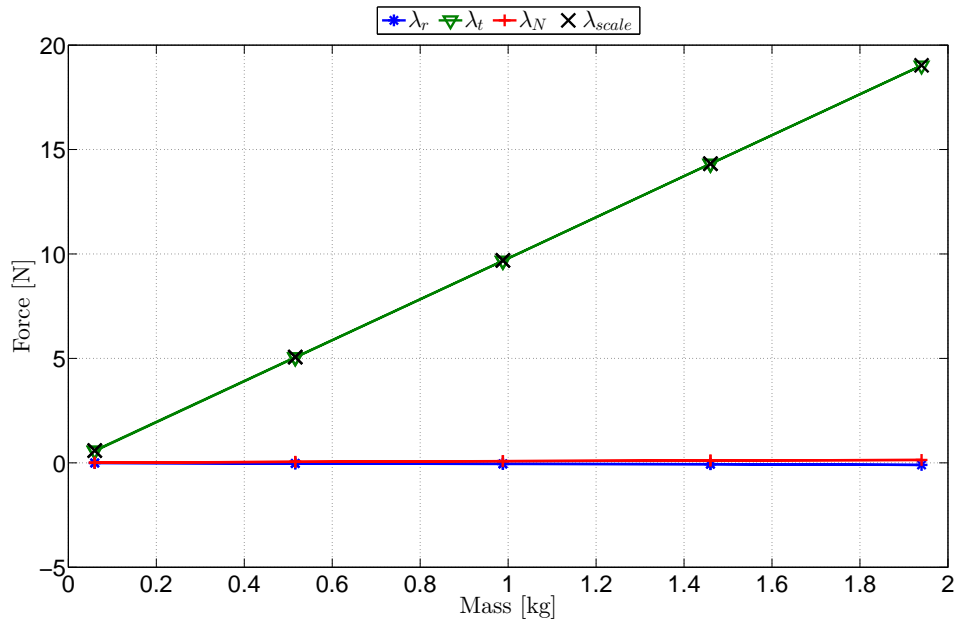


Fig 5.6: Forces measured in the S frame converted to the I frame with the force exerted in the \mathbf{e}_t^I direction.

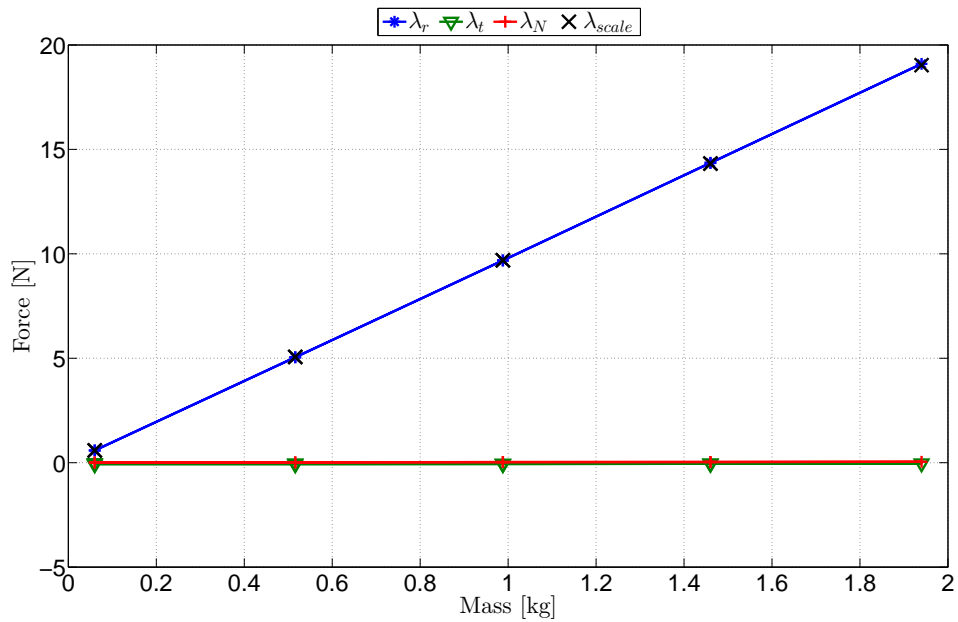


Fig 5.7: Forces measured in the S frame converted to the I frame with the force exerted in the \mathbf{e}_r^I direction.

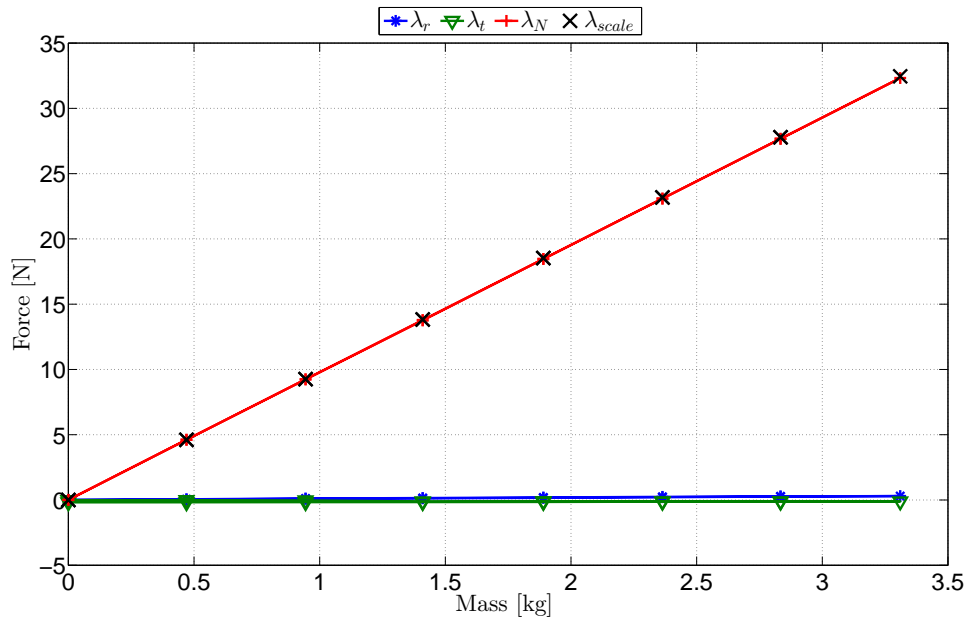


Fig 5.8: Forces measured in the S frame converted to the I frame with the force exerted in the \mathbf{e}_N^I direction.

5.3 Summary

This chapter first of all described the problem regarding the measured data. By applying known forces in known direction it is concluded that the sensor coordinate frame S is not orthonormal and thus not as expected (orthogonal to the sensor housing). Therefore a transformation is obtained from the sensor frame to the desired coordinate frame I . This is done by applying known forces in all directions of frame I and measuring the forces in the sensor frame. From this a transformation matrix is obtained from the force vector in the sensor frame to the desired force vector, this transformation matrix is given in Equation 5.7.

6 Other identified potential problems

This chapter discusses other observations which might influence the obtained results. First of all, the fact that a moment is applied instead of a pure force on the sensor is investigated. Thereafter, a change in measured values after turning on the setup is discussed. Furthermore, the fact that the friction force decreases for increasing velocity at low velocities is discussed. This is a phenomenon referred to as the Stribeck effect [5], [6]. Finally, the phenomenon of a high pitched noise coming from the setup is described.

6.1 Applied moments

The friction force is applied on the tip of the pin. Thereby, an arm is introduced due to which a moment is applied to the sensor. In this section it is tested if this has an influence on the measured data.

To test this, measurements are performed. These measurements are done by applying a constant force but different moments in radial and tangential direction. To do so a new pin is designed which has different grooves, see Appendix D. By hanging a constant weight from the different grooves a constant force is applied which creates different moments.

For these experiments a mass of 516 g is used to apply the constant force. Figures 6.1 and 6.2 show the change in measured force by increasing the arm length. In these figures the difference between the force measured with an arm length of 12 mm and the other arm lengths are displayed. The legend shows in which direction the force is applied in the I frame. The figures show that the difference in measured force in tangential direction is very small and thus negligible. But there is a clear linear change in measured force in radial direction of about 0.004 N/mm for the given applied force. For now it is assumed that this is negligible because the arm for the real experiments is about 12 mm and thus this would mean that the difference due to the applied moment is small.

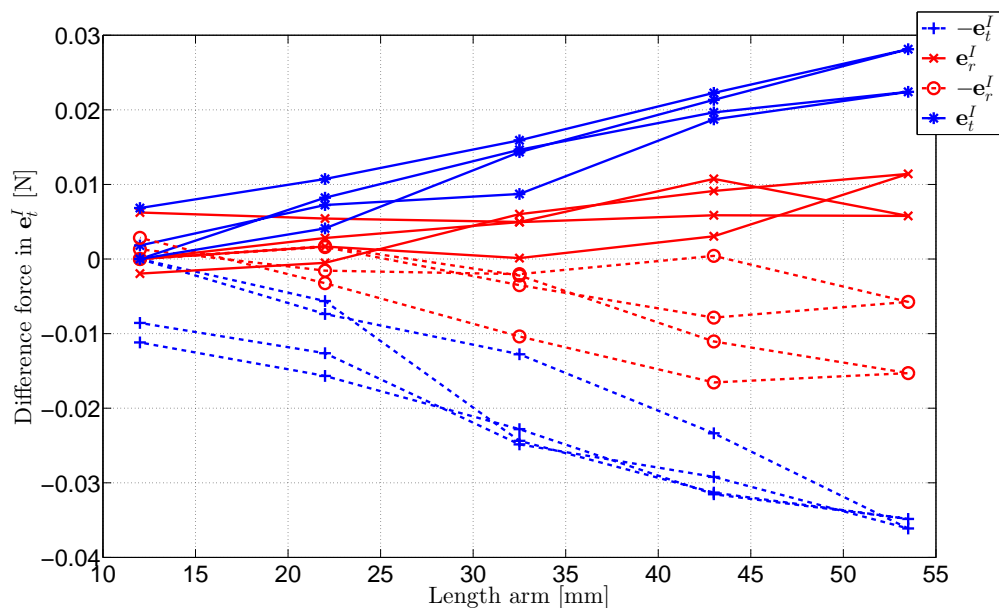


Fig 6.1: Change in measured force in the tangential direction dependent on the arm length of the pin. The used mass to apply the moments is 516 g.

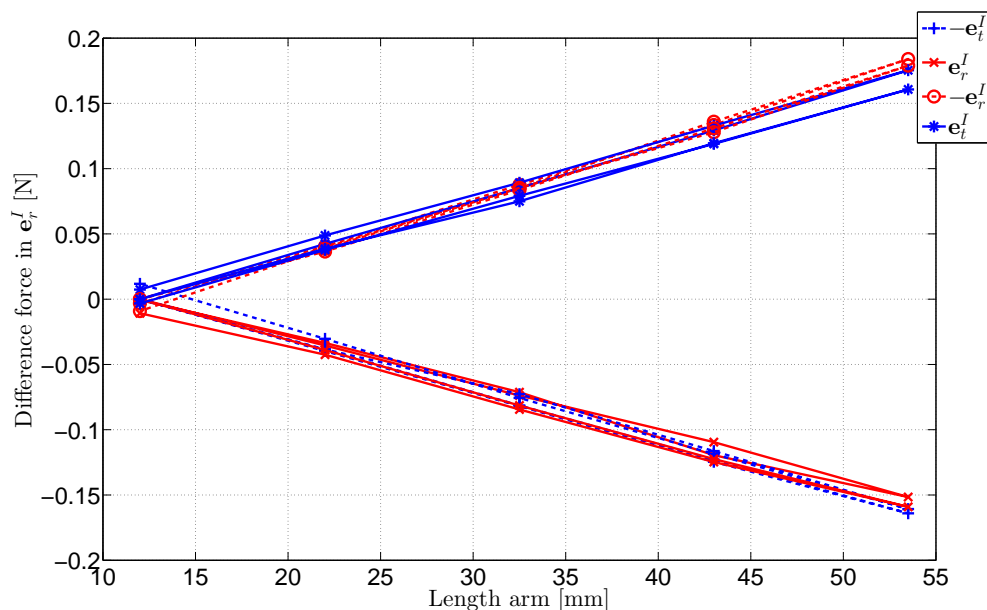


Fig 6.2: Change in measured force in the radial direction dependent on the arm length of the pin. The used mass to apply the moment is 516 g.

6.2 Startup of experiment

This section briefly discusses the change in measured values over time when the equipment is turned on. It is observed that when the equipment is just turned on, the measured values change over time. This might be caused by parts in the amplifier or force sensor heating up. In Figure 6.3 the forces in the S frame are shown when a brass pin is hanging from the sensor, with force measurements about one minute apart. It shows the offset of the sensor and clearly shows a change over time. From this it is concluded that at least 30 minutes before conducting a measurement everything has to be turned on. In the future it might be useful to send a known signal into the amplifier to check if this changes over time when amplified. This way it can be determined if the problem is caused by the amplifier or by the force sensor.

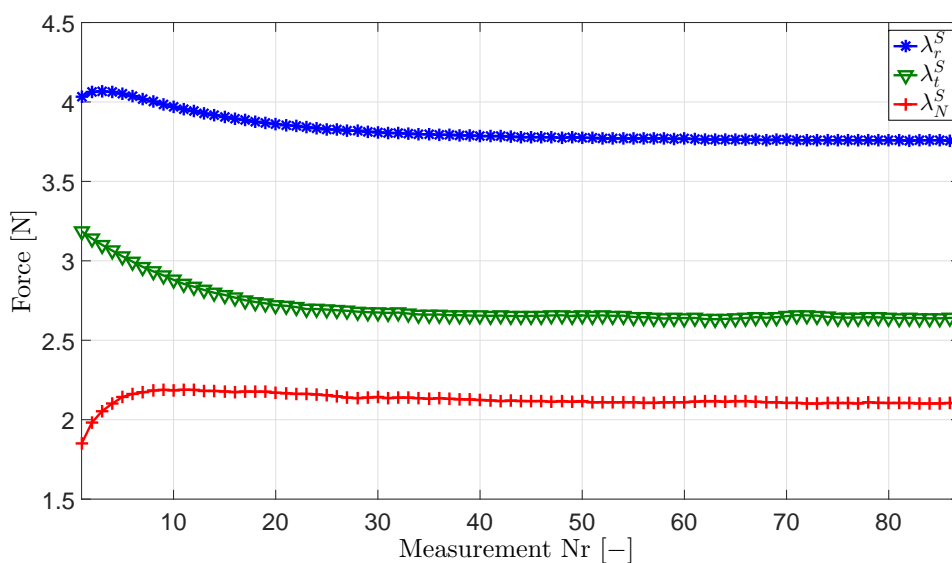


Fig 6.3: Change in measured forces when the equipment is turned on. The measurements are about one minute apart.

6.3 Stribeck effect

It is observed that for increasing sliding velocity the friction force decreases. Therefore, experiments are done using a brass pin on a sandblasted steel plate (isotropic) with different weights and sliding velocities. For every velocity the plate did two full rotations, the resulting mean value of the tangential (frictional) force is presented in Figure 6.4. The legend in this figure gives the cumulative weight of the slider and the added plates. From this figure is concluded that for the used materials a Stribeck curve is obtained. It is important to take this into account when doing measurements, because this clearly has an impact on the measured friction forces. This means that the assumption of Coulomb friction might not be valid, because the friction force is decreasing for increasing velocity. Which means that for different velocities, different force reservoirs are obtained.

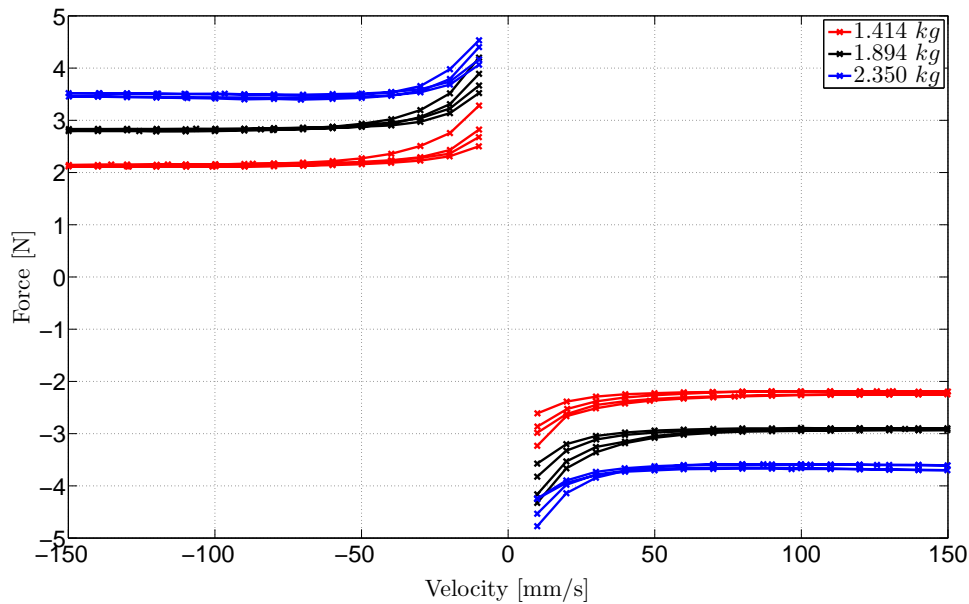


Fig 6.4: Frictional force for increasing sliding velocity in the I frame. A clear decrease in frictional force is shown for increasing velocity at low velocities.

6.4 Vibrations

For certain settings the setup produces a high pitched noise. This noise is most likely produced by vibrations. The decrease of friction force due to high frequent vibration is broadly discussed in literature [7], [8]. Therefore, the cause of this noise is investigated.

To investigate this sound the vibration of the force sensor is checked. It is tested if this vibration is a translation of the sensor or a rotation of the sensor. This is done by aiming a laser which measures velocity at different positions of the sensor. For one experiment the laser is pointed close to the center of the sensor (P_1) and in the other experiment is pointed at the edge of the sensor (P_2), see Figure 6.5. If it is a rotation around the normal axis, the velocity at P_2 should be much higher than the velocity at P_1 .

The velocity in both experiments is given in Figure 6.6. This figure shows that the velocity at P_2 is much higher than the velocity at P_1 . From this is concluded that the vibration is a rotation around the normal axis.

Now it is concluded that the vibration of the sensor is a rotation, it is checked if the produced sound is coming from this vibration. This is done by comparing the signal of the force sensors rotation and the sound coming from the setup. When computing the amplitude spectrum of both measurements they should have a peak at the frequency of the observed sound. The resulting amplitude spectrum for an experiment with both the microphone and the laser is shown in Figure 6.7. Because both amplitude spectra show a peak around 2040 Hz it is most likely that the sound

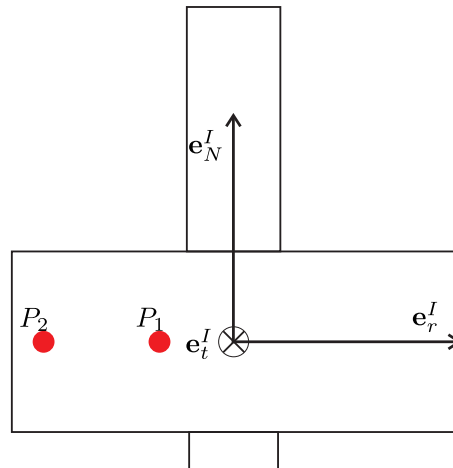


Fig 6.5: Laser position to determine if the vibration is a rotation or a translation.

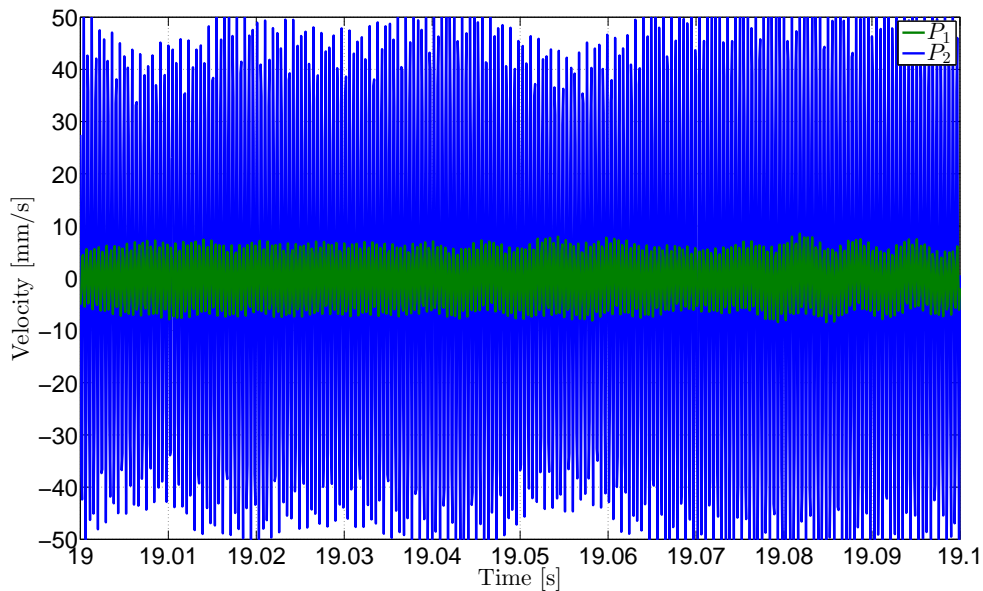


Fig 6.6: Velocity at P_1 and P_2 during experiment.

is caused by this vibration. In literature it is broadly discussed that high frequent vibration might cause a decrease in friction force [7], [8]. Therefore, this has to be further studied and has to be taken into account when taking future measurement.

6.5 Summary

In this chapter some potential problems of the setup are discussed. First of all, the fact that a moment is applied to the force sensor instead of a pure force. For now it is assumed that the influence on the measured force is negligible. Thereafter, the change of measured values when turning on the setup is analyzed. From this is concluded that the setup has to be turned on at least 30 minutes before doing experiments. Then, a decrease in friction force for increasing velocity is observed. This phenomenon is known as the Stribeck effect. This has to be taken into account in future research, while up to now Coulomb friction is assumed. Finally, a high pitched noise coming from the setup is analyzed. This noise seems to come from a rotation of the the force sensor around its normal axis. This has to be further studied while high frequent vibration might cause a decrease in friction force.

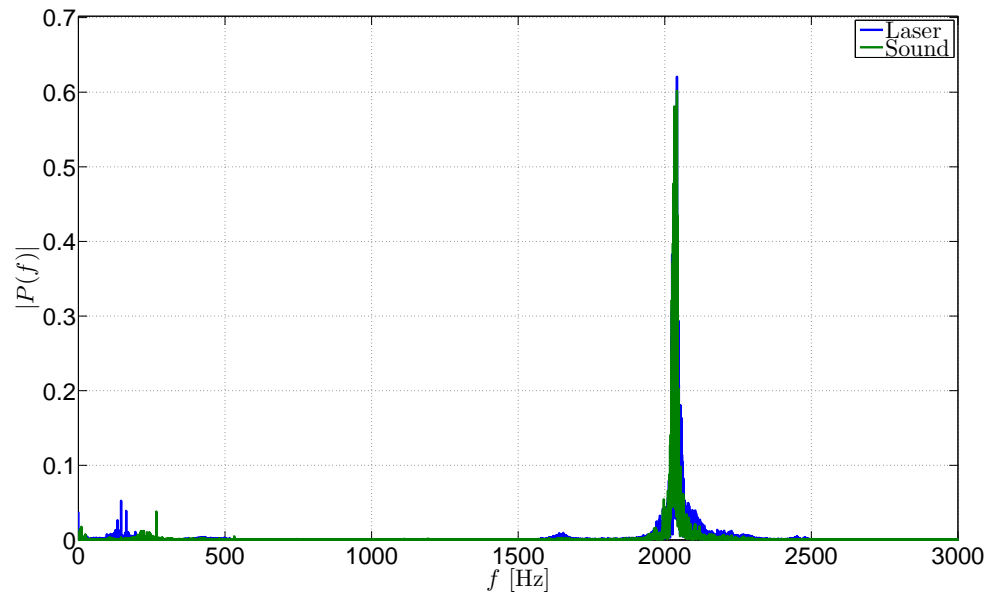


Fig 6.7: Amplitude spectrum of the sound and the velocity of the sensor.

7 Results of data transformation

This chapter shows the results when applying the obtained improvement of Chapter 5. It shows how the raw data is transformed for the measurement in Figure 5.1. Furthermore the change in force reservoir and direction set is shown. This is first of all shown for the isotropic example of Figure 5.1. Thereafter the same is shown for a measurement of an anisotropic specimen.

7.1 Isotropic results

This section shows the change in results due to the data transformation given in Chapter 5 for the previously used measurement of an isotropic surface. In Figure 5.1 an offset in the radial force is shown. This data is transformed from frame S to frame I which results in Figure 7.1. It shows that the radial force in frame I is much closer to zero. In Table 7.1 the mean values of all forces in frame S and I are given. It shows that in the I frame the mean of the radial force is close to zero.

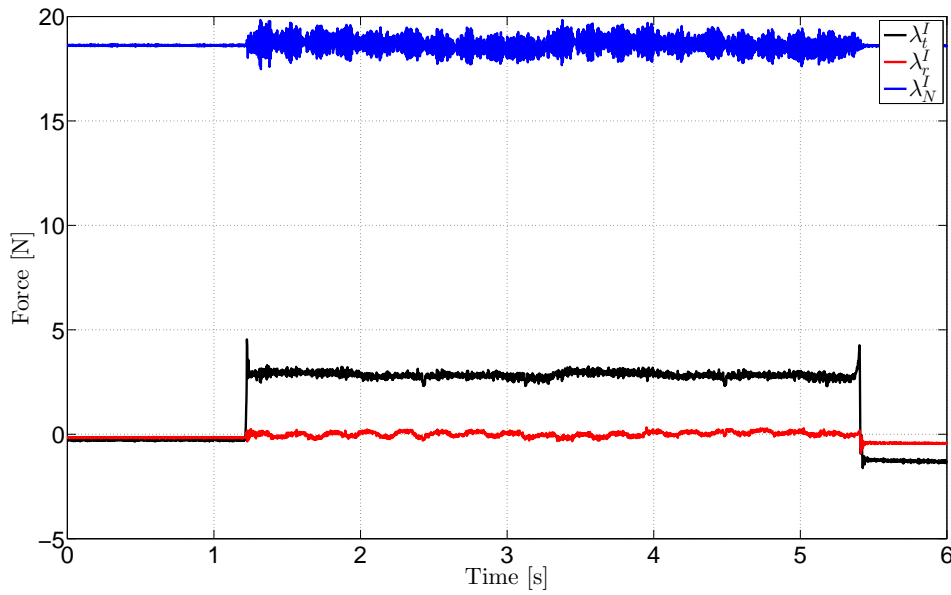


Fig 7.1: Raw measured forces transformed to frame I of an isotropic surface.

Table 7.1: Mean measured forces in frame S and I for two rotation with an isotropic surface.

Frame	λ_r [N]	λ_t [N]	λ_N [N]
S	0.963	2.840	18.50
I	0.006	2.839	18.66

The goal of the setup is to experimentally obtain the sets \mathcal{C} and \mathcal{D} . It is expected that these sets are closed, Figure 7.2 clearly shows that set \mathcal{D} is not closed, this is due to the offset in the radial force. The force reservoir looks like a circle which is expected for an isotropic material because the magnitude of the friction force is the same in every sliding direction. The forces shown in the figure are rotated to the directions λ_{T_1} and λ_{T_2} as given in Figure 3.2. This data is transformed to frame I before it is rotated to λ_{T_1} and λ_{T_2} which results in Figure 7.3. This results in a closed contour for both sets and both sets are almost perfect circles. For an isotropic surface two concentric circles are the expected result, because the direction of the friction force should be opposite to the sliding direction and the force should have a constant magnitude.

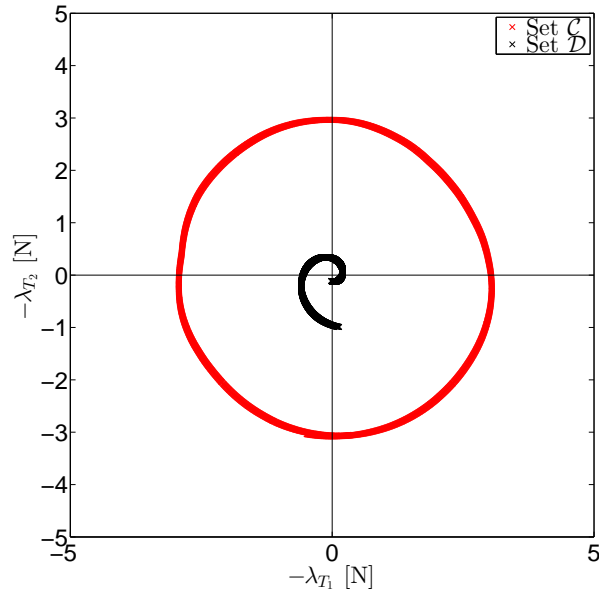


Fig 7.2: Sets \mathcal{C} and \mathcal{D} with the forces in frame S rotated to λ_{T_1} and λ_{T_2} .

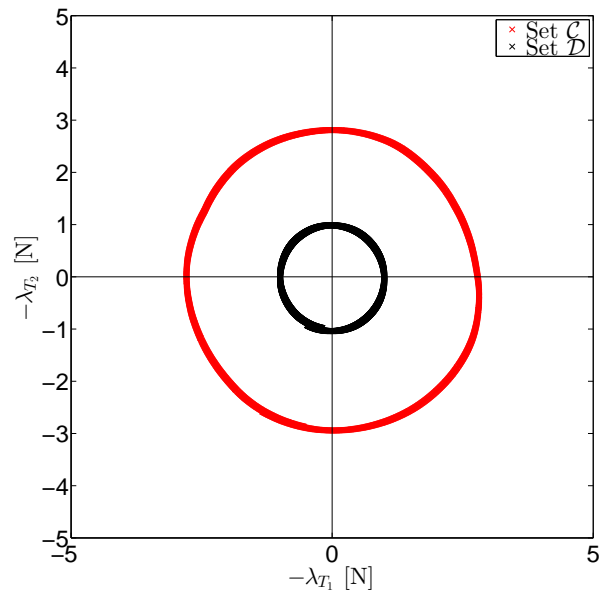


Fig 7.3: Sets \mathcal{C} and \mathcal{D} with the forces in frame I rotated to λ_{T_1} and λ_{T_2} .

7.2 Anisotropic results

In this section results are shown of a measurement of an anisotropic specimen because this is the reason the setup is developed. For this measurement a surface ground steel plate is used with all scratches in the same direction which results in an anisotropic surface and the used pin is made from steel.

The conducted experiment is done over four rotations and the measured forces in the I frame are shown in Figure 7.4. This figure shows that the normal and tangential force are fairly constant over a rotation but the radial force has a sawtooth shape. This is caused by the scratches, when the radial force is zero the scratches are moving parallel or orthogonal with respect to the pin.

The resulting force reservoir and direction set are shown in Figure 7.5. For this figure the data

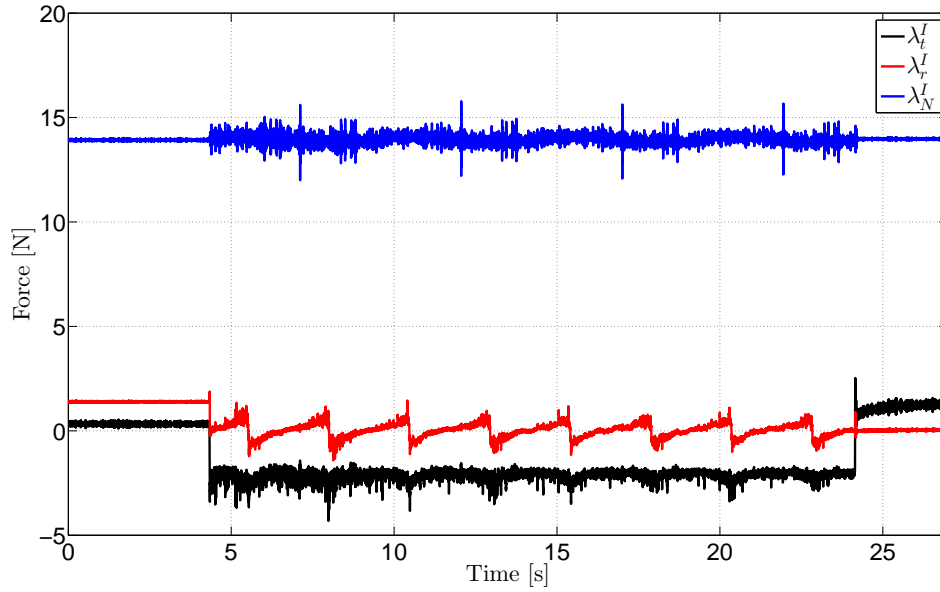


Fig 7.4: Measured forces transformed to frame I for an anisotropic surface.

is first transformed to the frame I and then rotated to the body fixed frame of the plate. It shows an almost closed direction set and a force reservoir which is different in shape. This figure shows anisotropic friction because the friction force is not the same for every sliding direction. The magnitude and direction are sliding direction dependent. It shows at the most far ends horizontal and vertical that the force direction is opposite to the velocity. Which means that at every $\frac{1}{2}\pi$ rotation the pin is sliding along with the scratches or orthogonal to the scratches.

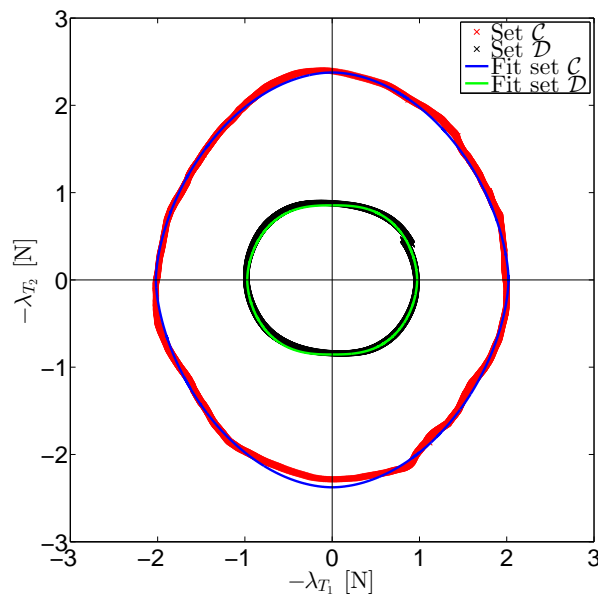


Fig 7.5: Resulting sets of the forces in Figure 7.4 with the fitted ellipses over the force reservoir and directions set.

Figure 7.5 shows that the superellipses are quite a good representation of both sets in this case. The mean distance between the fit and the contour of the force reservoir is 0.0281 N and 0.0173 for the direction set. The parameters of the superellipses are given in Table 7.2.

Table 7.2: Parameters of the fitted ellipses in Figure 7.5.

Parameter	Set \mathcal{C}	Set \mathcal{D}
m	1.883	2.758
n	1.683	1.804
a	2.020	0.973
b	2.376	0.854

7.3 Summary

This chapter shows the results of the data transformation from Chapter 5. This is done for an isotropic surface and an anisotropic surface. The resulting force reservoir and direction set are as expected. Furthermore, the fitting tool is tested on the force reservoir and direction set, it is concluded that for the used data the fit is a good representation of the sets.

8 Conclusion and recommendations

In this chapter first the conclusions from this project are given and then recommendations are done for follow up research.

8.1 Conclusion

The main goal as given at the beginning of the project is: Automating and improving the experimental setup. The part regarding the automation of the setup is achieved as described in Chapter 4. To achieve this goal a Matlab GUI is developed. This GUI can be used to do experiments as well as the post processing. Furthermore, the GUI contains a fitting tool to get a mathematical approximation of the force reservoir and the direction set. The improvement of the setup by a data transformation is explained in Chapter 5. A transformation matrix is obtained to transform the obtained data from the non-orthonormal sensor frame S to the desired frame I orthogonal to the sensor housing. With this data transformation some experiments are conducted as shown in Chapter 7. From these experiments is concluded that the obtained data transformation solves the problem of the non-orthonormal sensor frame. Furthermore, in Chapter 6 some other potential problems are described. For these problems no solution is found so it is important to take these into account in future research. All together it can be concluded that the main goal is achieved, experiments and post processing can be done using the GUI and the setup is improved in the sense that the measured data can be transformed to the desired data.

8.2 Recommendations

Although the main goal of the project is achieved there is still room for improvement of the setup. First of all, the rotation of the specimen is not perfect. The specimen does not rotate exactly the number of desired rotations. So, this could be improved in the GUI. Furthermore, a homing button could be added to the GUI such that every experiment starts at exactly the same position of the specimen. The data transformation is also not perfect. It could be determined more precisely by applying the forces to determine the transformation matrix more perfectly in the desired direction. For future research it is also recommended to look into the problems addressed in Chapter 6. The problem with the moment that is applied to the force sensor instead of a pure force might be solved by a new pin design which introduces a shorter arm. The changing values after turning on the setup might be solved by using another amplifier. Furthermore, it is important to take a look at the assumption of Coulomb friction because the Stribeck effect is observed during experiments. Finally, the influence of the sensors vibration needs some further research because this might influence the friction force as well.

References

- [1] Walker, S. (2015). Anisotropic dry friction. [online] Available at: http://www.inm.uni-stuttgart.de/forschung/projects/project_walker/index.html [Accessed at 30 January 2017].
- [2] Walker, S. (2016, unpublished), *Experimental Investigation of Anisotropic Dry Friction*. INM, University of Stuttgart.
- [3] Groschopp BV Drives & More (2010). *Product manual RBD-325-4/6-S*.
- [4] Dewesoft GmbH (2015). *DEWESoft7 DCOM Manual*. Version: 1.1.0. 2015.
- [5] Woydt, M., & Wäsche, R. (2010). *The history of the Stribeck curve and ball bearing steels: The role of Adolf Martens*. *Wear*, volume 268, Issues 11-12, p. 1542-1546.
- [6] Stribeck, R. (1902), *Kugellager Für Beliebige Belastungen*. *Zeitschrift des Vereins Deutscher Ingenieure*, 46, p. 1341–1348.
- [7] Godfrey, D. (1967). *Vibration Reduces Metal to Metal Contact and Causes an Apparent Reduction in Friction*. *ASLE Transactions*, 10:2, p. 183-192.
- [8] Chowdhur, M.A., Helali, M. (2006). *The effect of frequency of vibration and humidity on the coefficient of friction*. *Tribology International*, volume 39, Issue 9, p. 958-962.

A Matlab implementation of the specimens rotation

This appendix explains how the rotation of the specimen is implemented in Matlab to automate the setup. To start rotating using Matlab just three lines are required, first a connection with the used port has to be made using the following two lines in Matlab

```
1 ObjectServo = serial('COM12','Terminator','CR','BaudRate',115200); % Setting up ...
   connection with right port
2 fopen(ObjectServo) % Open connection with servo-controller
```

which creates a serial port object which uses the terminator 'Carriage Return' and sets the baud rate to the value that the servo-controller is using. The terminator is a command which is used to end a command which is application dependent. The baud rate is the rate at which information is transferred in a communication channel which is also application dependent. The second line opens the serial port such that commands can be send over this port.

The commands used by ServoCommander are given in the product manual of the servo-controller [3]. There is just one command needed to set the velocity over the RS-232 port, this command is given by

$$0W : 00E3 : FFFFFFFF, \quad (\text{A.1})$$

in which $0W$ stands for write, $00E3$ stands for set point rotation speed using the RS-232 port and $FFFFFFF$ is the value to send which represents the desired velocity. $FFFFFFF$ consists of a hexadecimal number which is linearly related to the turning velocity. To find the relation between the velocity of the motor and the commands, ServoCommander is used. By inserting different rotational velocities and then requesting the command which is send to the servo-controller a linear relation is found. This relation is given by the following equations

$$\begin{aligned} V_{com} &= N_{high} + VF, \forall -126.5333 < V < -8.533, \\ V_{com} &= N_{low} + VF, \forall -8.533 \leq V < 0, \\ V_{com} &= VF, \forall V \geq 0, \end{aligned} \quad (\text{A.2})$$

in which V_{com} is the value which is send to the servo-controller for the desired velocity. $N_{high} = 16777216$, $N_{low} = 1048576$, $F = 122880$ and V is the desired rotation speed of the specimen in rounds per minute.

To convert V_{com} into a command for the servo-controller it is converted to its hexadecimal representation. This gives a value which is shorter then 8 digits. To finish it symbols are added at the front to make the command 8 digits long, the added symbols are zeros for positive velocities and F's for negative velocities.

The obtained command is send to the servo-controller using the following line in Matlab

```
1 fprintf(ObjectServo, '%s\r', '0W:00E3:FFFFFFF') % Command to set desired velocity
```

in which $FFFFFFF$ is replaced by the command for the desired velocity.

For experiments translational velocity is desired as input instead of rotation speed. Therefore, the input values for the GUI are translational velocity, radius and number of rotation. These values are used to compute rotational velocity and time. The command corresponding to this rotational velocity is send to the servo-controller, then after the rotation time has passed a command is send for rotational speed zero. The flowchart in Figure A.1 shows the step sequence for rotation of the specimen.

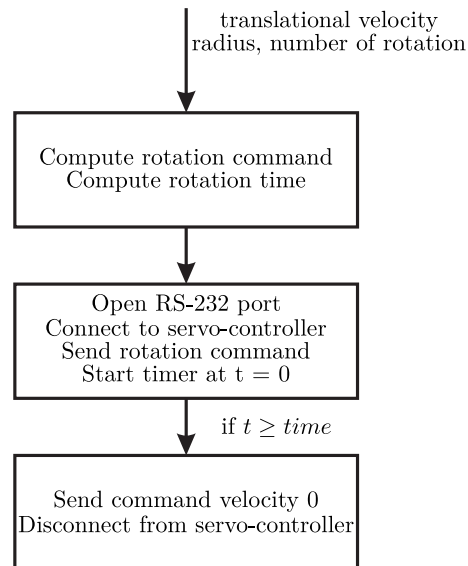


Fig A.1: Flowchart of the step sequence to rotate the specimen in the desired way using Matlab.

B Matlab implementation of the data acquisition

This appendix explains how the data acquisition is implemented in Matlab. The steps for data acquisition for an experiment are the following:

1. Connect with DeweSoft
2. Load a setup to tell DeweSoft which channels of the DEWE-BOOK to use
3. Reset force sensor to zero
4. Start acquisition
5. End acquisition
6. Export data to a '.mat' file

The first step, connecting to DeweSoft is done by the following lines in Matlab

```
1 h = actxserver('Dewesoft.App'); % Create a COM server which can be used to send ...
   commands to DeweSoft
2 h.invoke('Init')
3 h.Enabled = 1;
```

these lines make it possible to send DCOM commands to DeweSoft. To send DCOM commands DeweSoft does not have to be running but when it is running in the background everything works faster. Therefore, it is recommended to start DeweSoft before an experiment and to keep it running in the background.

The second step is to load a DeweSoft setup which contains the channels to use and the settings of these channels. This setup has to be created in DeweSoft manually and saved before an experiment. The setup is loaded using the following line in Matlab

```
1 h.LoadSetup(SetupName); % Load the setup
```

in this command SetupName is a string containing the name and location of the setup.

The third step is resetting the force sensors, this can be done if the settings in the setup are such that the three channels for the forces are on auto reset. Then, the following lines can be called in Matlab to do this

```
1 h.SetupScreen; % Go to the setup screen
2 h.ZeroAllAutoChannels(1); % Set auto reset channels to zero
```

the first line directs DeweSoft to switch to the setup screen, this is done because the reset button is in the setup screen environment. The second line calls the reset button and sets the three force channels to zero.

The fourth step is starting the data acquisition, this is done just before the motor starts spinning. To start the data acquisition the following commands are used

```
1 h.Measure() % Go to the measure screen
2 h.MeasureSampleRateEx = SampleRate; % Set sample rate
3 h.StartStoring(strcat(SaveName, '.dsd')) % Start storing data under defined name
```

the first line tells DeweSoft to go to the measure screen, the second line sets the sample rate to the desired value SampleRate and the last line starts the data acquisition under the desired location and name with the '.dsd' extension.

The fifth step is done after the rotation of the specimen, the acquisition of data is stopped and the data is saved as a '.dsd' file. This is done with one line in Matlab

```
1 h.Stop(); % Stop data acquisition and save data as '.dsd' file
```

this command represents the stop button in DeweSoft and stops the data acquisition and saves it under the chosen name with the '.dsd' extension.

The sixth and final step is to export the acquired data as a '.mat' file which can be used for post processing. This is done with the following lines in Matlab

```
1 h.LoadFile(strcat(SaveName, '.dsd')); % Load '.dsd' file from measurement
2 h.ExportData(3,2,strcat(SaveName, '.mat')); % Export loaded data to '.mat' file
```

the first line loads the data that has been obtained during the measurement. The second line exports the data under the same name and location, but with the '.mat' extension. The first integer defines the data format, in our case '.mat'. The second integer defines the format of the time axis, in this case the first sample is time instant zero. Using all these lines together makes it possible to acquire data using Matlab.

C GUI for experiments

This appendix shows a Figure of the final GUI created using GUIDE in Matlab.

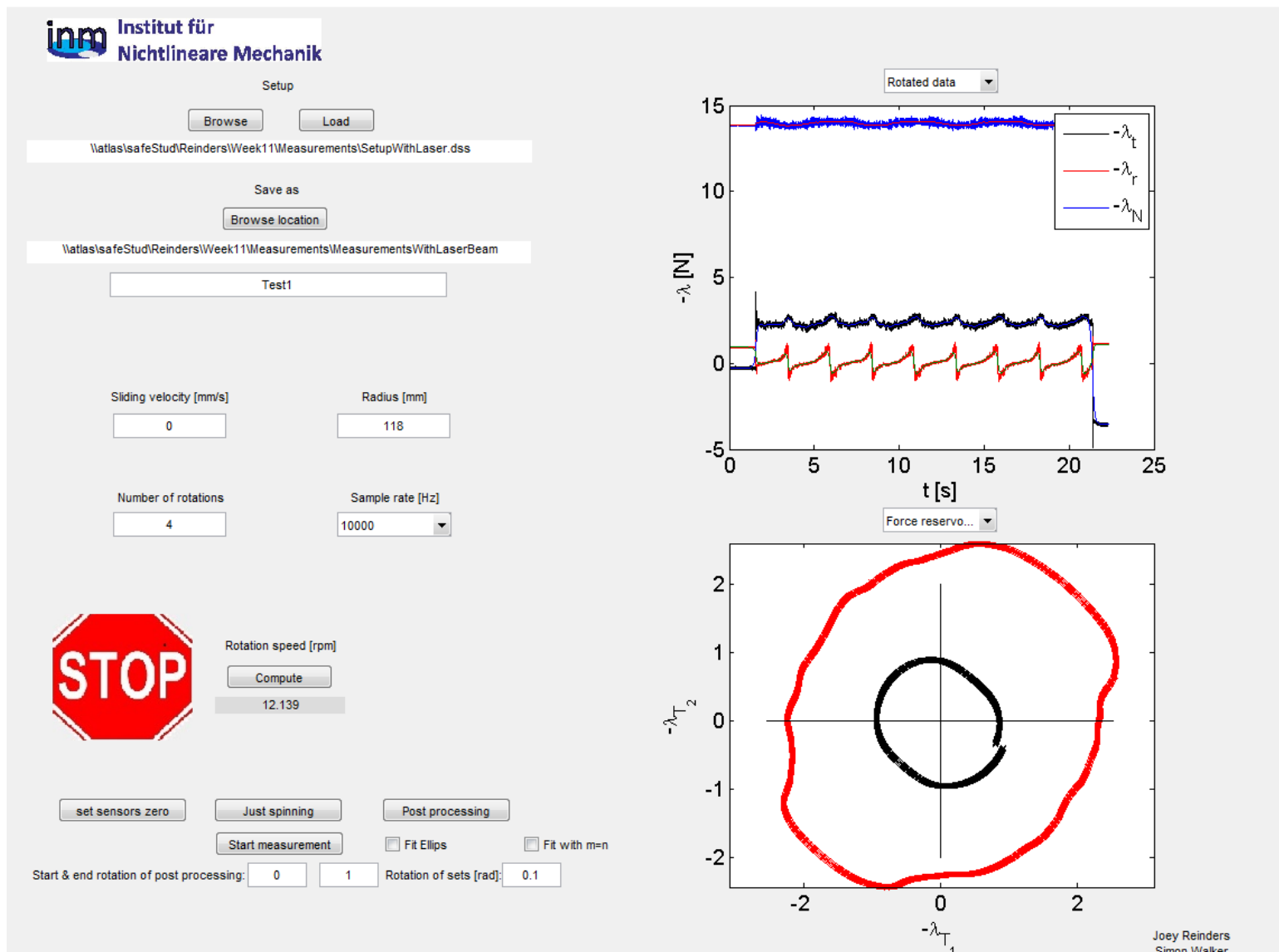


Fig C.1: The final GUI used to conduct experiments in Matlab.

D Applied moments

This appendix shows the figure of the pin used for testing the influence of the exerted moment on the measured force. The design of this pin is shown in Figure D.1.

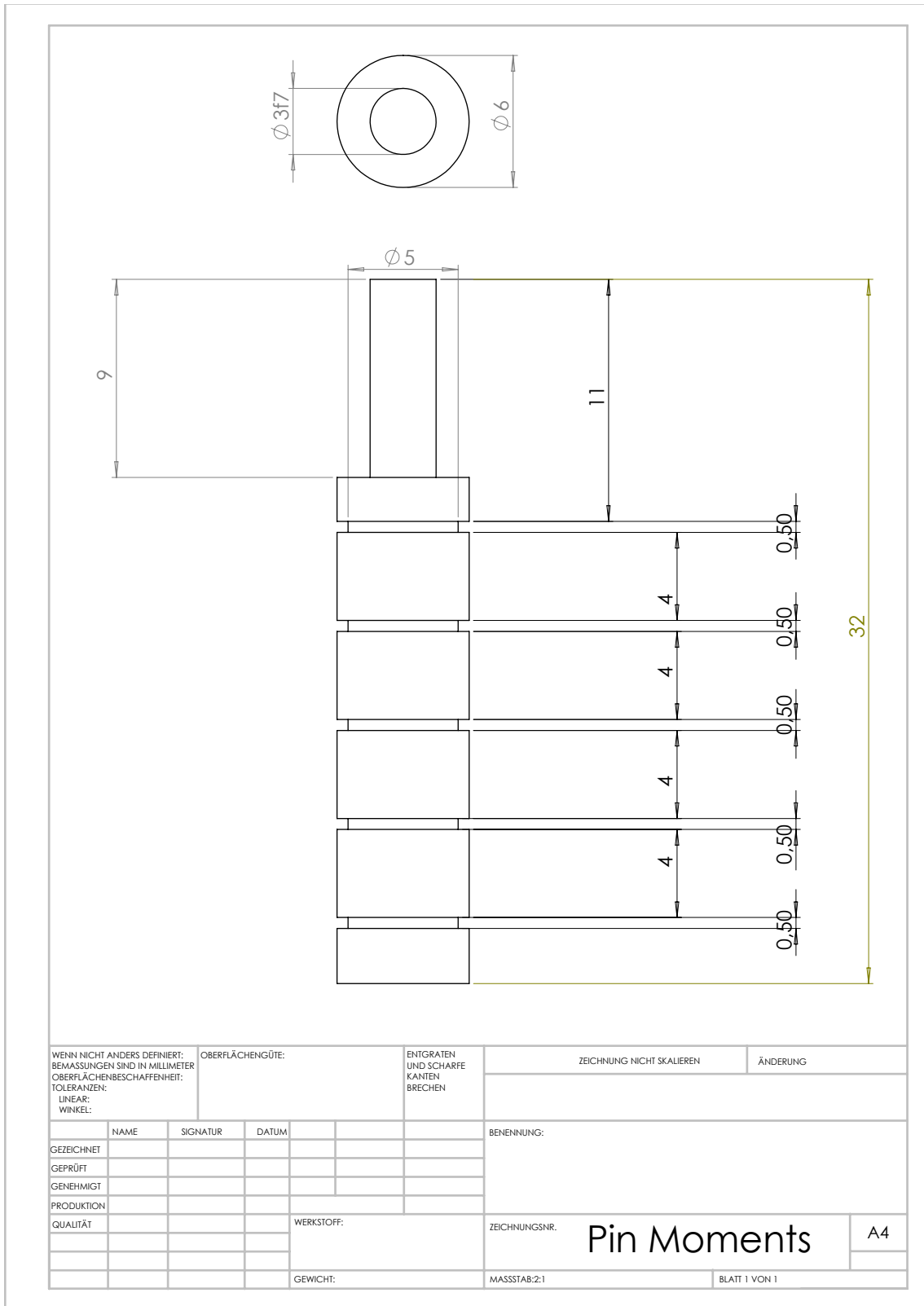


Fig D.1: The design of the pin used for testing the influence of the exerted moment on the measured force.